

Title: Topological Phase Diagram: Topological Embedding of Structural Brain Networks.

Authors: Moo K. Chung, Camille Garcia-Ramos, Nagesh Adluru, Bruce P. Hermann, Aaron F. Struck

ISMRM Annual Meeting 2025 #958

**Motivation:** Structural brain networks often tend to remain stable across both healthy and clinical populations, displaying minimal localized connectivity differences.

**Goals:** We introduce a novel data embedding technique designed to reveal and amplify subtle network variations that might otherwise go undetected.

**Approach:** By projecting network variations into a 2D topological space, our method significantly enhances the ability to discriminate between groups, making it possible to detect extremely subtle network differences that may be overlooked in traditional analyses.

**Results:** Using the proposed embedding technique, we were able to discriminate between 79 temporal lobe epilepsy (TLE) patients and 44 healthy controls.

**Impact:** Our novel topological embedding technique enhances the detection of subtle brain network differences, potentially improving diagnosis and understanding of neurological conditions. It enables researchers to investigate overlooked variations, opening new avenues in brain connectivity and disease characterization.

**Data and Preprocessing:** Diffusion-weighted MRI scans were acquired using 3T GE MR750 scanners; detailed information regarding image acquisition is available in Chu et al. (2023). The dataset consists of 79 temporal lobe epilepsy (TLE) patients and 44 healthy controls (HC). Tractography was performed using MRtrix3 to obtain connectivity edge weights between regions defined by the 164-region Destrieux atlas in FreeSurfer. Fifteen million streamlines were generated through dynamic whole-brain seeding using fiber orientation distributions (FOD) and the probabilistic algorithm iFOD2, which performs second-order integration over FOD. These anatomical cortico-subcortical gray matter regions served as the nodes in the networks. The edge weights were determined by the cross-sectional areas (CSAs) of the underlying white matter fiber bundles connecting pairs of nodes. The CSA of each fiber bundle was calculated as the total sum of iteratively optimized weights that represent the fidelity of fiber tracts compared to the measured diffusion signal. These edge



comparisons correction. As a result, we might incorrectly conclude that there are no group differences.

**Topological Phase Diagram (TPD):** To address this challenge, we propose embedding the structural connectivity into topological phase diagrams (TPDs) using persistent homology, a powerful multiscale algebraic topology method for characterizing underlying topology of data (Chung et al. 2024). We embed each subject-level connectivity matrix into a 2D plane, where the x-axis represents the average birth values of 0D topology (connected components), and the y-axis represents the average death values of 1D topology (cycles) (Figure 2).

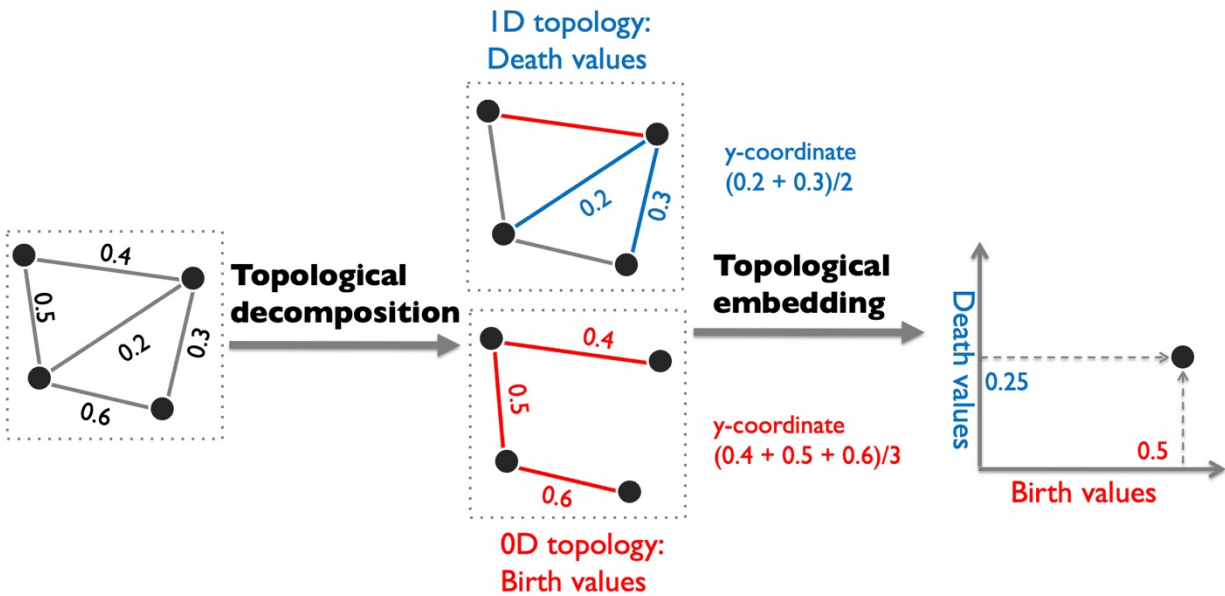


**Figure 2.** Schematic of the proposed topological embedding. Weighted networks go through topological decomposition, where 0D and 1D topologies are split orthogonally. Edges corresponding to the birth of 0D topology (connected components) form the maximum spanning tree (MST), while edges corresponding to the death of 1D topology (cycles) form the non-MST edges. The average birth (x-coordinate) and average death (y-coordinate) values of these edges are used as coordinates in the topological embedding.

The topological embedding reveals clear group separations (Figure 3-right). Squares represent the topological means of each group, while circles indicate individual networks. Contour plots display the distribution of networks in the embedding space, with networks in the upper right expected to be more complex than those in the bottom left. HC networks are predominantly distributed with larger birth and death values compared to TLE

networks, indicating that healthy controls exhibit more persistent topological features in both connected components (0D topology) and cyclic structures (1D topology). This suggests that the structural brain networks of healthy individuals have greater complexity and robustness, with topological features that persist over a wider range of thresholds during the analysis. In contrast, TLE networks display smaller birth and death values, reflecting less persistent or fewer topological features, which may be associated with disruptions or simplifications in brain connectivity. These differences highlight the effectiveness of our topological embedding in distinguishing between the two groups by capturing subtle variations in network topology that traditional methods might overlook.

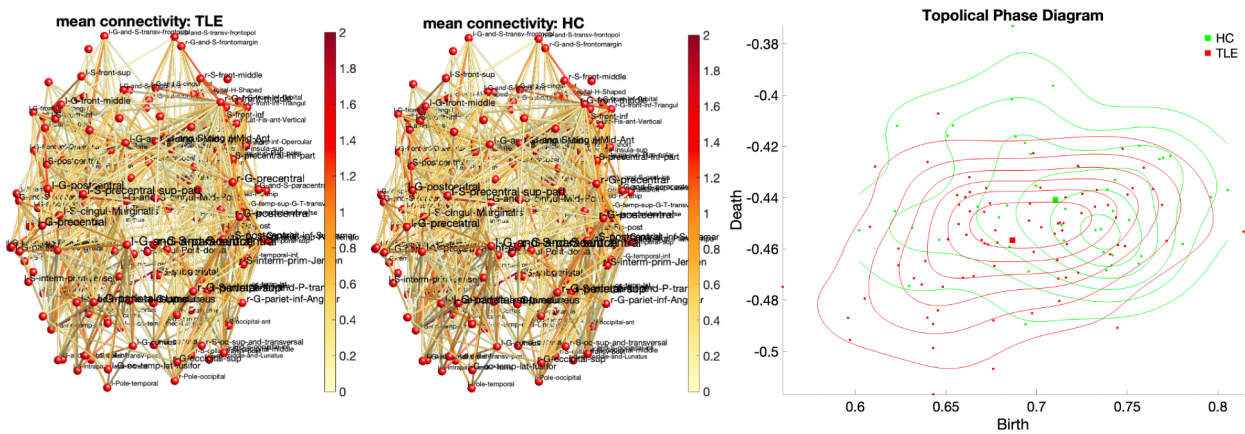


**Figure 3.** Mean connectivity in 79 temporal lobe epilepsy (TLE) patients and 44 healthy controls (HC). The connectivity patterns are highly stable across groups, with no detectable differences. As a result, one might incorrectly conclude that there are no group differences. However, the topological phase diagram clearly reveals group separation in both 0D (birth) and 1D (death) topology. Squares represent the topological centroids of each group, while contours represent kernel density estimates, illustrating the distributional patterns.

**Topological Inference:** The group separation observed in the TPD is statistically quantified by calculating the topological distance between networks (Chung et al. 2023). For a collection of networks in the TPD, the topological distance  $d(X, Y)$  between two networks  $X$  and  $Y$  is defined as the sum of the squared differences in their birth and death values. The between-group distance is then computed as the sum of all  $d(X, Y)$ , where  $X$  belongs to the TLE group and  $Y$  belongs to the HC group. A larger between-group distance, or equivalently a smaller within-group distance, suggests that the two groups are more topologically distinct, making this metric useful as a test statistic. Then the test statistic is determined by the ratio of the between-group and within-group distances (Figure 4). By comparing the between-group distance to the within-group variability, this ratio effectively normalizes the

measure, enhancing the detection of significant topological differences between the groups.

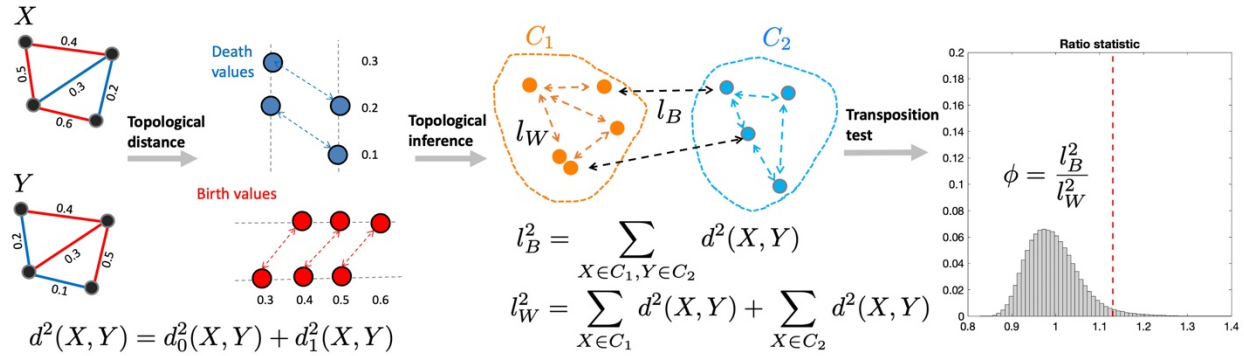


**Figure 4.** Schematic of the proposed topological inference. We first compute the topological distance as the sum of the discrepancies of the 0D and 1D topological features, measuring the differences in connected components and cyclic structures. Then we compute the between-group and within-group distances. The online permutation test is then conducted using the ratio statistic of between-group to within-group distances.

The p-value ( $p = 0.0156$ ) was computed by generating 100 million permutations to approximate the null distribution, a process that took only 40 seconds on a desktop computer. To expedite the computation, we utilized the transposition test—an online permutation test that iteratively updates the test statistic by sequentially permuting only one subject per group. During each transposition, the between-group and within-group distances are sequentially updated using only the terms that involve the transposed subjects in each group. While traditional permutation tests require recomputing the test statistic at each permutation, the transposition test updates the previously estimated test statistic with incremental changes. This approach significantly speeds up the permutation process.

**Acknowledgements.** This study was supported by NIH U01NS093650, NS117568, EB028753 and NSF MDS-2010778.

Reference.

Chu et al. (2023) Association of neighborhood deprivation with white matter connectome abnormalities in temporal lobe epilepsy, *Epilepsia* 64:2484-2498.

Chung et al. (2023) Unified topological inference for brain networks in temporal lobe epilepsy using the Wasserstein distance. *NeuroImage* 284:120436

Chung et al. (2024) Topological embedding of human brain networks with application to dynamics of temporal lobe epilepsy. *ArXiv* 2405:07835